Lightning surges in hybrid cable-overhead lines. Part I: Voltage estimation for shielding failure

Silva, Filipe Miguel Faria da; Pedersen, Kasper

Published in:
Electrical Engineering

DOI (link to publication from Publisher):
10.1007/s00202-022-01538-z

Publication date:
2022

Document Version
Accepted author manuscript, peer reviewed version

Lightning surges in hybrid cable-overhead lines. Part I: Voltage estimation for shielding failure

F. Faria da Silva[a,]*, Kasper Pedersen[b]
[a] *AAU Energy Technology, Aalborg University, Pontoppidanstræde 111, 9220 Aalborg, Denmark*
[b] *DanGrid, Sanderumvej 16B, 5250 Odense, Denmark*
**Corresponding Author: E-mail: ffs@energy.aau.dk*

Abstract

The increasing usage of hybrid cable-overhead lines raises concerns over the protection of short cable sections against lightning surges, because of voltage build-up in the cable section. To set a simulation model of the phenomenon is time consuming, with numerous parameters impacting the overvoltage.
This paper (Part I) presents formulas able to perform a fast estimation of the maximum overvoltage at a cable-overhead line transition point in the event of shielding failure. The formulas estimate the overvoltage with and without surge arrester, as well as the energy absorbed by the surge arrester. These formulas do not require an Electromagnetic Transients (EMT) software and they can be implemented as a script, requiring solely the geometric data of the cable and overhead line, information available in the respective datasheets. The main usefulness is a tool for a fast screening of the overvoltages and a fast evaluation of the impact of different parameters such as cable length, lightning waveform and grounding impedance.

Keywords: Lightning; HVAC cables; Surge arrester; Insulation coordination; Screening tool

I. Introduction

With raising public opposition to the construction of new overhead lines (OHL), the installation of underground cables has been steadily increasing. Underground cables have higher purchase and installation costs than equivalent OHL, and the combination of the two technologies in one line (a so-called hybrid-line or syphon-line) is an interesting choice that allows limiting cable sections to locations likely to raise public objections, as the crossing of nature surroundings or populated areas, per example.
Lightning surges on hybrid lines might propagate from the OHL phase conductors or earth wires into the cable phase conductors or sheaths, respectively. Depending on the length, attenuation and terminations of the cable, multiple reflections can occur at the cable ends resulting in a voltage build-up. Additionally, the energy dissipated by a surge arrester at an OHL-cable junction increases, because of the aforementioned reflections.
To evaluate the impact of lightning surges on the cable sections of an hybrid line is not a straightforward task and it requires a high level of detail. Several factors affect the waveform: Corona in the OHL, grounding impedance of towers and cable sheaths, or attenuation along the cable. Furthermore, during the planning stage for a new installation, a high number of uncertainties exist and part of the data is unavailable. An EMT simulation is always more accurate and necessary if precise values are required, but to set an EMT simulation model accounting all factors is time-consuming, it requires human resources with specialised knowledge on EMT simulations and an EMT software tool. A screening tool in the style of IEEE-Flash [1], [2] would be helpful, by allowing both a fast assessment of the phenomenon severity, by varying a series of parameters that are uncertain at the earlier stages of a project (e.g. cable length, grounding impedance, surge arrester type), and by not requiring an engineer with expertise in insulation coordination. The results from the screening tool would allow to decide if a more detail assessment of the overvoltages is necessary. To develop the equations for such screening tool is the main objective of this paper.

Part I of this work presents formulas able to estimate the peak voltage at a cable core caused by a lightning surge hitting an OHL phase conductor (shielding failure). Additionally, the paper presents formulas able to estimate the energy dissipated in a surge arrester at a cable-OHL transition.

Section II summarises the basics of the phenomenon, Section III provides formulas for estimating various surges impedances at high frequencies, Section IV develops formulas for estimating the overvoltage in case of shielding failure and Section V considers the presence of a surge arrester at the joint point. Section VI discusses selected key results and Section VII concludes the paper.

II. Phenomenon description

Reference [3] from the same authors introduces the phenomenon in detail and summarises the potential impact of different parameters (e.g., Corona effect might be disregarded). Reference [4] studies the phenomenon for a real line and it shows that for the specific system shielding failure is not an issue, but a lightning surge at a transition tower or at an adjacent one can damage the cable. References [5] and [6] show that the maximum overvoltage might be along the cable and not at the terminations. Reference [6] proposed a method to estimate this location and value, but an EMT-type program is required for acquiring the input parameters. A summary of the phenomenon is presented next.

II.1. Shielding Failure

Typically, the surge impedance of a cable is several times lower than the surge impedance of an OHL with the same nominal voltage and similar ampacity. As a result, the crest value of a voltage impulse propagating from an OHL into a cable reduces when entering the latter, with the opposite happening when propagating from a cable into an OHL. The relation between voltages are given by (1), where V_I is the incident voltage, V_F is the voltage refracted forward, V_R is the voltage reflected back, Z_B is the characteristic impedance of the line to where the wave is propagating into and Z_A is the characteristic impedance of the line which the voltage wave is propagating from.

$$\begin{cases} V_F = V_I \dfrac{2Z_B}{Z_A + Z_B} \\ V_R = V_I \dfrac{Z_B - Z_A}{Z_A + Z_B} \end{cases} \tag{1}$$

The voltage reduction when a wave propagates into a cable has an initial positive impact, as the crest value reduces and the insulation stress is lower. However, if the cable is short, several reflections occur leading to a voltage build-up. Figure 1 shows the voltage at an OHL-cable transition point for two different cable lengths, an unloaded and unenergized cable and a 1.2/50 μs lightning impulse of 4 kA. The peak overvoltage is 4.8 times larger for the shorter cable, because of the voltage build-up caused by reflections at the cable terminals.

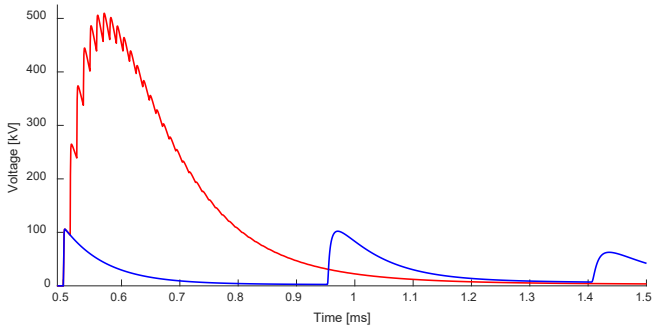

Figure 1 - Voltage at the transition point due to shielding failure. Blue: 40 km long cable; Red: 1 km long cable

II.2. Lightning hitting earth wire

The majority of lightning surges are expected to hit the earth wires. Afterwards, the propagation of the energy can be in one of two ways:

- I) the lightning current propagates into the ground and the cable sheaths;
- ii) a back-flashover occurs and there is current in both the phase conductors and the earth-wires.

These two sub-cases are studied in Part II.

III. Surge impedance estimation for high frequencies

The estimation of the crest voltage without an EMT-type software is divided into several steps, starting with the estimation of the cable and the OHL surge impedances, for two reasons:

- To convert the lightning current magnitude into a voltage at the OHL;
- To estimate the reflection/refraction coefficients between OHL and cable.

The first reason is valuable for assessment studies: The cumulative frequency of lightning peak current together with recommendations for modelling the waveshape have been published by CIGRE; the most recent reference is [7], but the majority of the main results were originally provided by [8]. This data can be an input for a statistical analysis. The second reason is necessary for estimating the voltage build-up.

The surge impedance of a cable or of an OHL at power frequency is often available at the respective datasheet or it can be easily calculated, as capacitance, inductance and resistance are provided. However, the phenomenon of interest in this paper relates with lightning surges and short cables. Therefore, the frequencies of interest are high and power frequency values cannot be used.

Simplifications can be done when calculating the surge impedance for high frequencies:

1. The resistance can be neglected, as the reactance dominates, with the surge impedance approximated by (2);

$$Z_0 = \sqrt{\frac{L}{C}} \tag{2}$$

2. The capacitance is mostly frequency independent for both OHL and cables;
3. The positive-sequence inductance of OHLs and cables decreases as frequency increases. The formula proposed in [9] considers the complex depth of the earth return model and it can be used to account the frequency impact (3); where, h is the height, p is given by (4) and ρ is the ground resistivity;

$$L_{OHL}(f) = \mathrm{Re}\left(\frac{\mu_0}{2\pi}\ln\left(\frac{2(h+p)}{GMR}\right)\right) \tag{3}$$

$$p(f) = \sqrt{\frac{\rho}{j\omega\mu_0}} \tag{4}$$

4. If the frequency is high enough, (3) simplifies into (5), with a small error in the estimation of the voltage.

$$L_{OHL} = \frac{\mu_0}{2\pi}\ln\left(\frac{2h}{GMR}\right) \tag{5}$$

5. For high frequencies, each phase of a three-phase single-core cable behaves similar to a coaxial cable, as the sheath acts as shielding. In these conditions, the positive-sequence inductance is given by (6), where R_1 and R_2 are the radius of the core and insulation, respectively;

$$L_C = \frac{\mu_0}{2\pi}\ln\left(\frac{R_2}{R_1}\right) \tag{6}$$

Given the large range of possible soil resistivity values, the disregarding of the complex depth in step 4 must be further analysed. The error due to the simplification increases as the soil resistivity increases. For the OHL considered in this paper, the error from the simplification is inferior to 2% for a soil resistivity of 20 Ω.m and frequencies above 40 kHz, increasing to 6% for 100 Ω.m and to 21% for 10000 Ω.m. As a result, the error associated to the simplification is not negligible when estimating the inductance for a high soil resistivity. However, the final objective of the paper is to estimate

an overvoltage, not the inductance of an OHL, and the error reduces substantially when doing the former. As an example, for an exaggerated high soil resistivity of 10000 Ω.m, the 21% error in the estimation of the inductance reduces to 11% for the OHL surge impedance. As it will be shown, the surge impedances are used to calculate the refraction OHL-cable coefficient, where the error reduces to 10%, and the cable reflection coefficient, where the error reduces to 3%. For a simulation like the ones done later in this paper with a 10000 Ω.m soil resistivity and a 1km long cable, the difference in the estimated overvoltage from not considering the penetration depth is 4%. This percentage reduces as the soil resistivity reduces. Further considerations on the impact of the soil resistivity are made in Section VI.

In summary, the characteristic impedances of OHL and cable are calculated using (2), with the capacitance of cable and OHL obtained from the datasheet directly, and the inductance of OHL and cable calculated by (3)-(5) and (6), respectively.

IV. Lightning Hitting Phase Conductor (Shielding Failure)

IV. 1. Formulas

The worst-case is to have a lightning surge hitting an OHL phase or a tower/earth-wire next to the OHL-cable transition point, as there is no damping along the OHL. This case is considered in the paper and wave attenuation along the OHL is neglected.

Equation (7) estimates the peak voltage at the lightning hitting point, where I_L is the lightning peak current and Z_{OHL} is the surge impedance of the OHL. The first peak voltage at the cable sending end (V_{H_C}), i.e. without reflections, is given by (7) multiplied by the OHL-cable refraction coefficient ($k_{O\text{-}C}$) (8). If no reflection occurs, the voltage at the cable sending end due to lightning (V_{Base}) is given by (9), where k, α and β depend on the selected double exponential wave.

$$V_H = \frac{I_L}{2} Z_{OHL} \tag{7}$$

$$V_{H\_C} = V_H \cdot k_{O-C} \tag{8}$$

$$V_{Base}(t) = V_{H\_C} \cdot k\left(e^{-\alpha t} - e^{-\beta t}\right) \tag{9}$$

To account the several reflections, the voltage at the cable sending end (V_{Send}) is estimated by adding V_{Base} and a cumulative of voltage reflections. Equation (10) estimates the voltage at the instant the wave is reflected at the junction point into the cable, after being reflected at the receiving end, i.e. the first reflection at the cable sending end. Where, n corresponds to the number of the reflection, A is the wave attenuation in the cable, l_C is the length of the cable, k_{Rec} is the reflection coefficient at the receiving end and k_{Send} is the reflection coefficient at the sending end.

$$V_{Send}(n=1) = V_{Base}(n=1) + \frac{V_{H\_C}}{e^{2A \cdot l_C}} \cdot k_{Rec}\left(1 + k_{Send}\right) \tag{10}$$

V_{Base} is calculated for the time instant corresponding to the reflection n, which requires knowing the propagation speed in the cable (11). This velocity changes for low frequencies, but it is mostly steady for the frequencies of interest and approximated by (12), where c_0 is the speed of light in vacuum and ε_r is the relative permittivity of the cable main insulation.

$$t(n) = n \cdot \frac{2l_C}{v_C} \tag{11}$$

$$v_c = \frac{c_0}{\sqrt{\varepsilon_r}} \tag{12}$$

The reasoning behind (10) is extended for further reflections (13): W_{Front} (14) is the front of the voltage wave after being reflected n times, whereas *diff* (15) is the cumulative summation of all previous reflections with the respective attenuations. The deduction of the formulas is available in appendix.

$$V_{Send}(n) = V_{Base}(n) + W_{Front}(n) + diff(n), \text{ if } n \geq 2 \tag{13}$$

$$W_{Front}(n) = \frac{V_{H\_C}}{e^{n(2A \cdot l_C)}} \cdot \left(k_{Rec} \cdot k_{Send}\right)^n \left(1 + \frac{1}{k_{Send}}\right) \tag{14}$$

$$diff(n) = \left(1 + \frac{1}{k_{Send}}\right) \cdot \sum_{z=2}^{n} \frac{V_{Base}(n-z+1)}{e^{(2A \cdot l_C) \cdot (z-1)}} \left(k_{Rec} \cdot k_{Send}\right)^{z-1} \tag{15}$$

The variables W_{Front} and *diff* account for the attenuation of the waveform, otherwise the voltage would increase indefinitely after each reflection. The attenuation is equal to the real part of the propagation constant (16), where the L_C is assumed to be for high frequency and thus, constant and given by (6). The resistance R_C increases continuously with frequency and it can be estimated by (17), using a formula from [10], where R_1 is the radius over the cable core, ρ_c is the conductor resistivity and μ_0 is the permeability in vacuum. The frequency for (16) and (17) is estimated by (18) [11].

$$A(f) = \mathrm{Re}\left(\sqrt{\left(R_C(f) + j\omega L_C\right) \cdot \left(j\omega C_C\right)}\right) \tag{16}$$

$$R_C(f) = \frac{R_1 \sqrt{\frac{\mu_0 \rho_c \omega}{8}} + \rho_c \frac{277}{777}}{\pi R_1^2} \tag{17}$$

$$f = \frac{v_c}{4 l_c} \tag{18}$$

Figure 2 shows V_{Send} and the other variables of (13) for a 1.2/50 µs waveform and a 1000 m long cable, with the maximum overvoltage occurring for the seventh reflection.

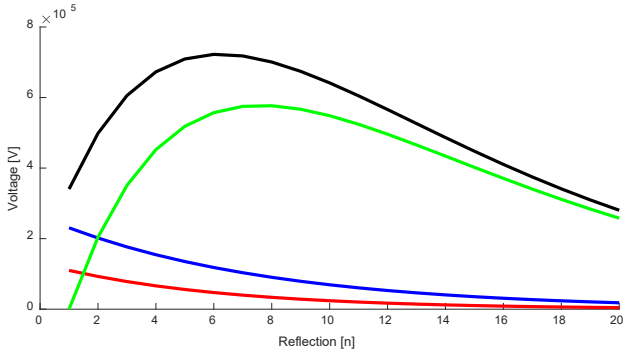

Figure 2 – V_{Send} (black), diff (green), W_{Front} (blue) and V_{Base} (red) for a 1.2/50µs lightning impulse and a 1000m long cable

Figure 3 summarises all steps required for estimating the peak voltage at the cable sending end at each reflection. The ending condition is the estimation of the maximum overvoltage. If desired, a fixed number of iterations can be defined, to estimate the voltages after the peak.

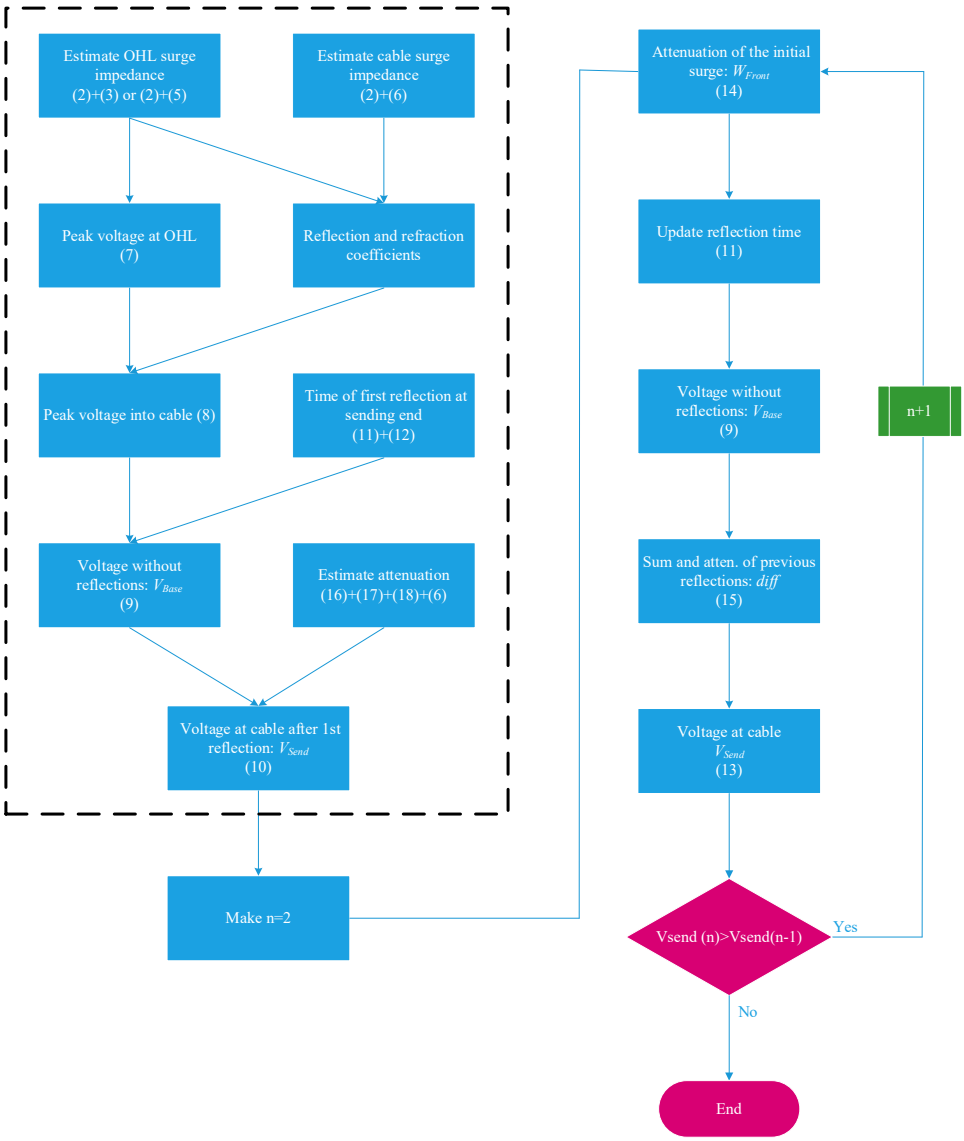

Figure 3 – Flowchart summarising calculation of voltage at the cable sending end for shielding failure. The number between brackets correspond to the number of the equation in the paper

IV.2. Validation

The proposed formulas are compared with results obtained using PSCAD/EMTDC. A full geometric three-phase circuit representation of the cable and OHL via frequency-dependent models considering couplings between conductors is implemented. The data used in the model and a simplified equivalent diagram are presented in Appendix.

Figure 4 shows the peak voltage at the respective reflection instant for a 1.2/50 µs lightning impulse of 5 kA and three different cable lengths: 500 m, 1000 m and 2000 m. For simplicity, the system is unloaded, the only energy source is the lightning impulse and the cable is open at the receiving end. The current magnitude is not relevant for this validation and a magnitude of 5 kA is selected randomly as being a realistic value for shielding failure. Figure 5 shows the relative error of the proposed formulas when compared with the simulation for four different double exponential curves: 1.2/50 µs, 2.6/50 µs, 5/320 µs and 8/20 µs. As expected, the error tends to increase as the number of reflections increases and errors accumulate. For the 1.2/50 µs impulse, the error of the peak voltage is below 4% for the three cable lengths, with similar results obtained for the 2.6/50 µs impulse. The error for the 5/320 µs impulse is of similar order for each reflection, but because this type of wave has the peak overvoltage at a latter instant, the error of the peak voltage is bigger.

The 8/20 µs impulse presents larger error. This happens because the raising and fall times are similar and the proposed method works on the principle that the raising time is much shorter than the falling time.

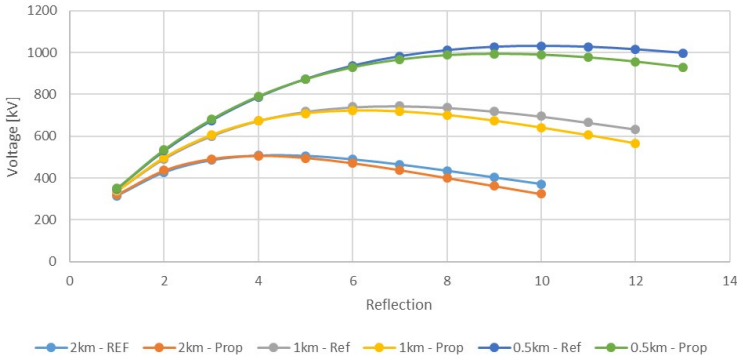

Figure 4 – Voltage for a 1.2/50 µs lightning impulse for different cable lengths, using the proposed formulas (Prop) and simulation in PSCAD/EMTDC (Ref)

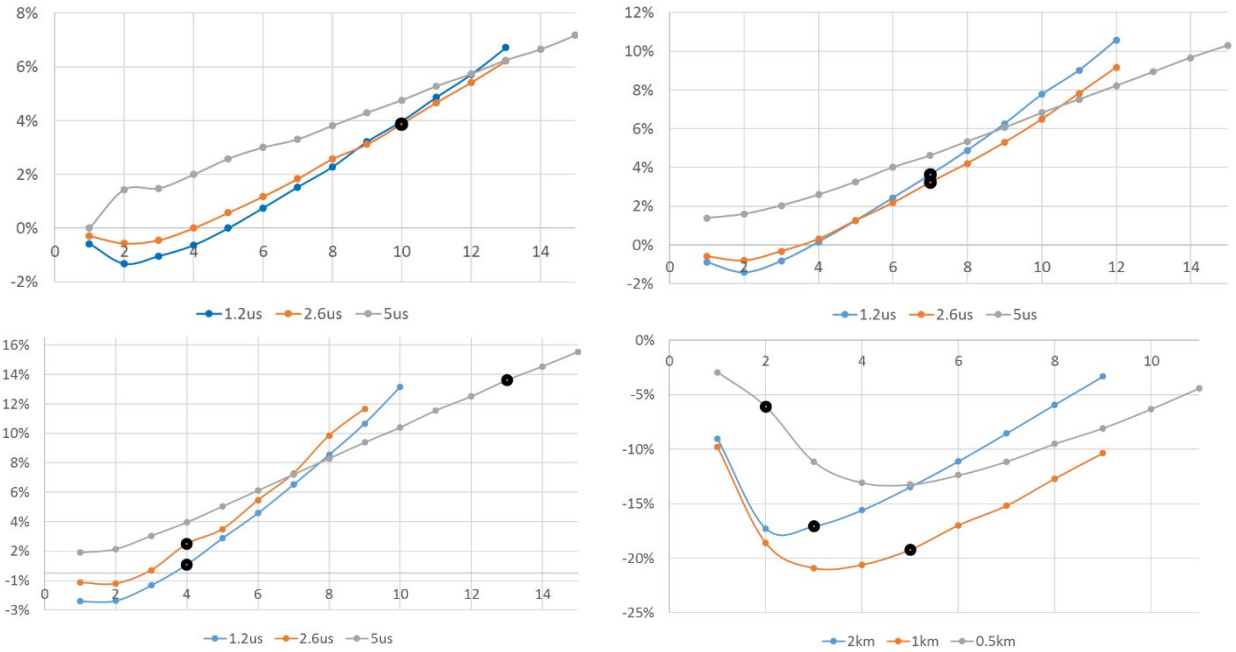

Figure 5 – Relative error of the proposed formula for different reflections. Top left: 500 m cable; Top right: 1000 m cable; Bottom left: 2000 m cable; Bottom right: cases for 8/20 µs, Black dots indicate the reflections corresponding to the maximum overvoltage

For a better validation, a second set of simulations is prepared. The front and time-to-half values recommended in [7] and [12] are employed to prepare a lognormal distribution of the lightning impulses. The measurements that were the foundation to recommend this lognormal distribution show a correlation of 0.25 between the front and the time-to-half of a negative stroke [13], which corresponds to a coefficient of determination (R^2) of 6.25%. As a result, the time-to-half is considered independent of the front time for this validation.

100 front times were considered with 10 time-to-half values, resulting in a total of 1000 simulations. The simulations are performed in PSCAD/EMTDC and the simulated peak voltage compared with the one obtained using the proposed formulas. The simulations are done for a 1km long cable and a lightning current of 5 kA. Figure 6 shows the error in the peak overvoltage when estimated by the proposed method, whereas Figure 7 shows the cumulative error.

The error increases with the increase of the front time, with approximately 85% of the cases having an error in the estimated peak overvoltage inferior to 10%. The reason for the error to increase with the front time is the method assuming an instantaneous rising time for estimating the variable V_{H_C}.

The impact of the time-to-half is mostly minor, except if its duration is similar to the front time, which might happen to the longest front times. As an example, for a front time of 30.06 µs, the error in estimating the peak overvoltage has an average of 26% and it varies between 20% and 34%, for time-to-half of 133.98 µs and 42.77 µs, respectively. This explains the larger error observed for the 8/20 µs waveshape.

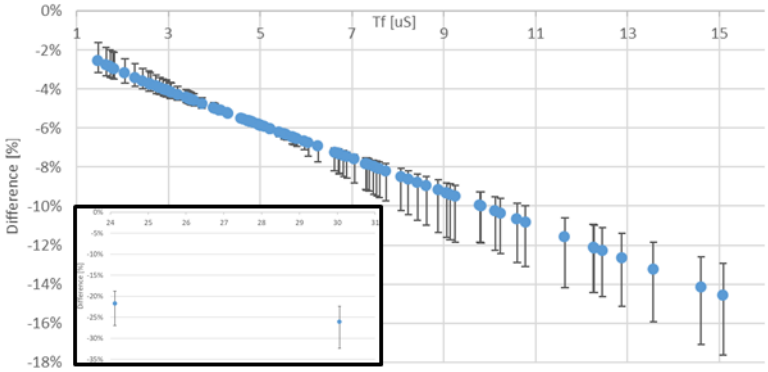

Figure 6 – Difference between peak overvoltage estimated via PSCAD simulations and via the proposed formulas for different front times. Blue dots are the average difference for each front time and the bar the positive and negative standard deviations for the time-to-half values

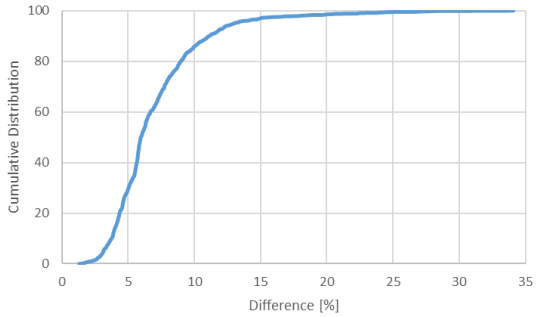

Figure 7 – Cumulative distribution of the difference between the estimated and simulated peak overvoltages

V. Impact of surge arrester

V.1. Description of Impact

The connection of a surge arrester at OHL-cable transition points for protection of the cable is common. This section proposes new equations able to account for its presence.

Different surge arresters modelling approaches exist: the IEEE-model [14], the CIGRE model [15], the Pinceti-Giannettoni [16] model or the Fernandez-Diaz model [17], with the latter two being simplifications of the first one, but easier to implement, because they do not require physical data on the surge arrester. Figure 8 shows the IEEE-model, consisting of two non-linear resistances (A_0 and A_1), separated by a low-pass filter. The design is such that for slow-front surges, the two non-linear resistances are in parallel, whereas for fast-front surges, the filter impact is more significant.

The frequency dependence of the filter and the non-linearity of the two resistances complicates the inclusion of a surge arrester in an analytical procedure, with simplifications being necessary.

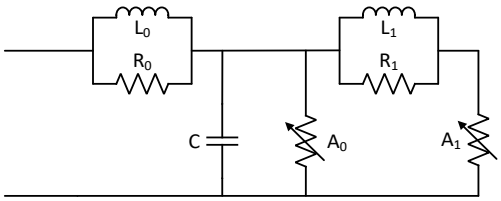

Figure 8 – IEEE Surge Arrester model

Reference [14] indicates that for a narrow range of time to crest values, the model may simplify into an inductance in series with a non-linear V-I characteristic. For the analytical method presented next, the surge arrester model simplifies further, becoming only the non-linear resistance with the values associated to A_1. The error associated to the simplification is acceptable for two reasons:

1. The limited current magnitude for shielding failure: Reference [18] shows that the maximum shielding failure current is usually below 20 kA for typical towers. It should be noticed that [19] shows that for EHV/UHV towers, the shielding failure is larger than estimated by traditional models, but these voltage levels are not considered in this work, as no cables operate at such high voltages, presently. Therefore, 20 kA is used as threshold, which limits the impact of the error, as the voltage magnitude at the junction point at the arrival instant is also limited.
2. The reflections occurring with surge arrester result in smaller voltage variations at the junction point. As a result, the simplified model presents a higher error for the high frequency oscillations at the first reflections, but it decreases as the phenomenon continues.

The values used for modelling a surge arrester should be tuned to the specific surge arrester. For this paper, the reference values given in [14] are used. The majority of the current tends to go to A_1, instead of A_0, except for very short times to crest, because of the filter (L_1//R_1). This means that a bigger error exists for faster front-times.

Figure 9 and Figure 10 show the voltage at the junction point and the current into the surge arrester for a 1.2/50 µs impulse. The figures show the simulated voltage and current with the IEEE surge arrest model, with a simplified model containing only A_1 and for a variation of the estimation method proposed in this paper and explained later. The results from the proposed estimation method follow are similar to those from the simplified surge arrester model, with both having similar differences to the reference IEEE model. The error reduces if the raise time decreases (Figure 11 shows an example for a 10 kA - 5/320 µs impulse), because of the lower relative current blocked by the low-pass filter, which increases the relative current flowing to A_1, instead of A_0. For all figures, the green curves should not be compared for all time-instants. The values are estimated only at the reflection instant, with the plot showing a linearization between these instants.

Extra simulations were performed for different cable lengths and lightning impulses. The tendencies are similar to those present here. Figure 12 shows the error in the estimated peak overvoltages for different waveforms, according to the lognormal distribution recommended in [7] and [12], alike the previous section. Contrary to the cases without surge arrester, the error decreases as the front time increases, because of the lower relative current blocked by the low-pass filter.

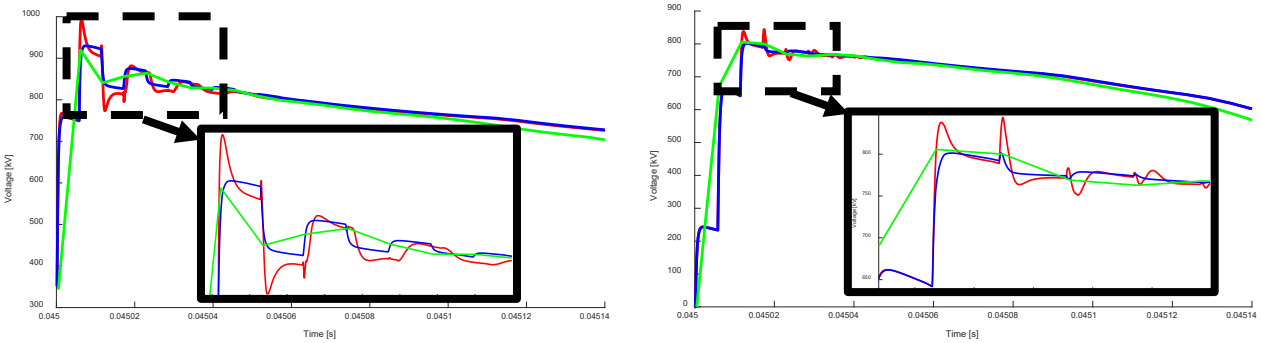

Figure 9 – Voltage at the junction point. Red: IEEE surge arrester model; Blue: Only A_1; Green: Proposed estimation method. Left: 20 kA lightning impulse and peak voltage at the phase; Right: 10 kA lightning impulse and 0 V at the phase

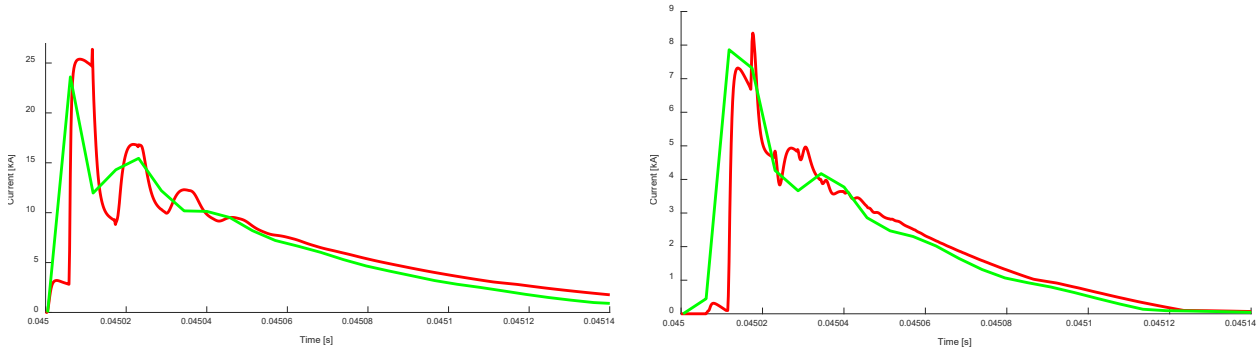

Figure 10 – Current into the surge arrester: Red: IEEE surge arrester model; Green: Proposed estimation method. Left: 20 kA lightning impulse and peak voltage at the phase; Right: 10 kA lightning impulse and 0 V at phase

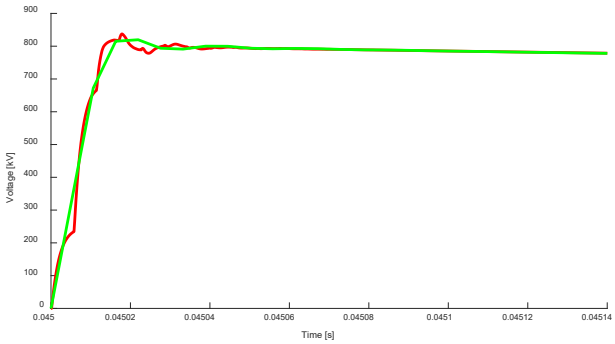

Figure 11 - Voltage at the junction point for 10 kA – 5/320 µs lightning impulse and 0 V at phase: Red: IEEE surge arrester model; Green: Proposed estimation method

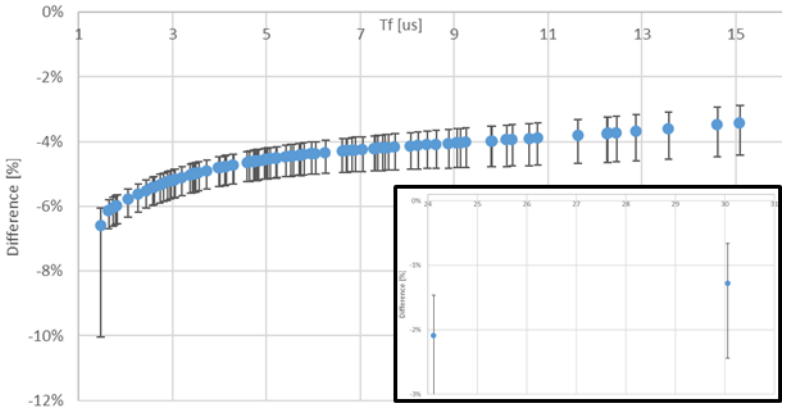

Figure 12 - Difference between peak overvoltage estimated via PSCAD simulation and via the proposed formulas for different front times. Blue dots are the average difference for each front time and the bar the standard deviation from the time-to-half values

The equations presented next are able to perform a fast estimation of the energy dissipated by the surge arrester during the transient. Figure 13 shows the energy absorbed by the surge arrester for two different cable lengths (0.5 km and 2 km), a 20kA - 1.2/50 µs lightning impulse and phase voltage at peak or at 0 V at the lightning instant. The energy from the simulation is the one at variable resistor A_1, which dominates.

The estimation of the energy via the proposed formulas might be done via two different methods: To use the maximum voltage and current point of two consecutive reflections (Figure 13-left) or to average the voltage and current of two consecutive reflections (Figure 13-right). The latter tends to be more accurate, but there are cases with large variations at the reflection instant where the former is more accurate.

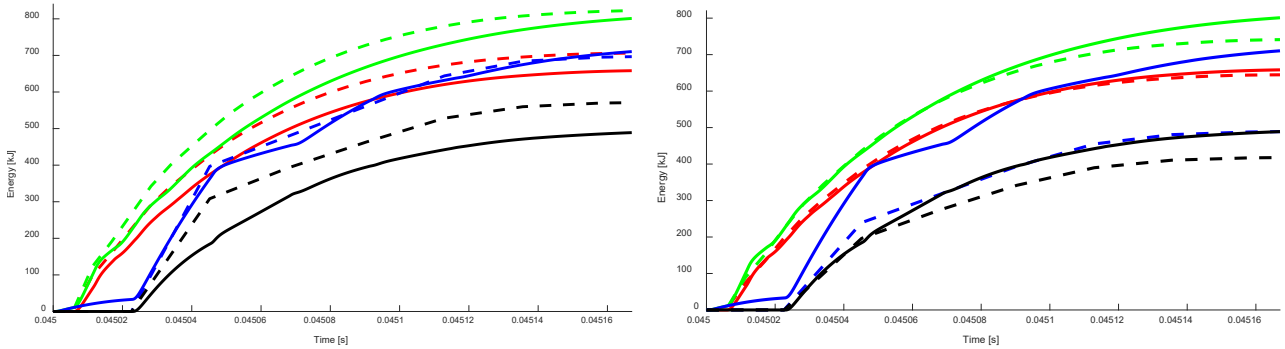

Figure 13 – Energy at surge arrester. Solid Lines: Simulation; Dashed lines: Proposed formulas. Left: Maximum energy between reflections; Right: Energy averaged between reflections. Green: 0.5 km cable and peak voltage at lightning instant; Red: 0.5 km cable and 0 V at lightning instant; Blue: 2 km cable and peak voltage at lightning instant; Black: 2 km cable and 0 V at lightning instant;

V.2. Changes to the estimation formulas

The estimation of the overvoltages considering a surge arrester is alike the method previously described with one extra step and variations in some of the formulas. If the surge arrester conducts, a new value for the current and voltage must be estimated. The non-linearity of the device leads to the estimation via the intersection of the V-I curve of A_1 with a curve built using the voltage at the joint point (V_{Send}) estimated via (13) and a current calculated from this value (19), where Z_C and Z_{OHL} are the surge impedances of the cable and OHL, respectively.

$$I_{Var}(n) = \frac{V_{Send}(n)}{\frac{Z_C \cdot Z_{OHL}}{Z_C + Z_{OHL}}} \tag{19}$$

Figure 14 exemplifies the methods, with the blue curve being the V-I curve of A_1, but with a linear scale for the horizontal axis instead of the typical logarithmic scale, and the orange curve being the one generated for estimating the operational point. The voltage value of the orange curve starting point is V_{Send} and the current of the ending point is I_{Var}. The voltage value at the crossing point of the two curves corresponds to the voltage at the joint point between OHL, cable and surge arrester.

The expression for estimating the voltage at the cable sending end is still (13), but the expressions for W_{Front} and *diff* require changes, in order to account the impact of the surge arrester on the reflected waves, resulting in a slightly changed expression (20). The difference is the partial replacement of k_{Send} by K_{Send_Arr} (21), leading to new expressions for W_{Front_Arr} (22) and *diffArr* (23). The deductions of the expressions are shown in the Appendix.

$$V_{Send}(n) = V_{Base}(n) + W_{Front\_Arr}(n) + diff_{Arr}(n), \text{ if } n \geq 2 \tag{20}$$

$$k_{Send\_Arr}(n) = \prod_{y=2}^{n} k_{Send}(n+1-y) \tag{21}$$

$$W_{Front\_Arr}(n) = \frac{V_{H\_C}}{e^{n(2A \cdot l_C)}} \cdot (k_{Rec})^n \, k_{Send\_Arr}(n)\left(1 + k_{Send}(n)\right) \tag{22}$$

$$diff_{Arr}(n) = \left(1 + \frac{1}{k_{Send}(n-1)}\right) \cdot \sum_{z=2}^{n} \left(\frac{V_{Base}(n-z+1)}{e^{(2A \cdot l_C) \cdot (z-1)}} (k_{Rec})^{z-1} \, k_{Send\_Arr}(n) \right) \tag{23}$$

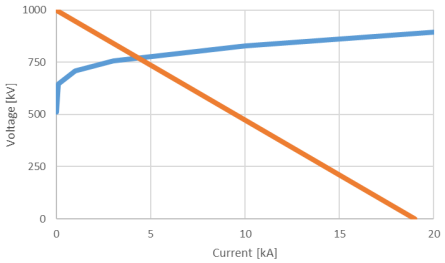

Figure 14 – Intersection between the V-I curve from A_1 (blue) and the curve generated from estimation method (orange)

VI. Discussion

VI.1. Insulation breakdown:

The proposed formulas estimate the voltage magnitude at the sending end of a cable and they can easily estimate it at the receiving end, if necessary. References [6] and [20] show that the maximum overvoltage might not be at the terminals, but along a cable. The latter reference proposes a method able to estimate this location, but it requires the voltage magnitudes at the cable terminals as inputs; both can be obtained using the formulas proposed in this paper. The voltage estimated via the formulas can be used for assessing insulation breakdown.

Insulation breakdown is not solely function of the voltage magnitude, but also of the waveshape [21]. The waveshape is similar to the ones in Fig. 4 and Fig. 5, with the reflection number replaced by the correspondent time instant, which can be estimated using (11). Figure 15 shows an example of the voltage at a cable sending end obtained via an EMT simulation (blue) and via the proposed formulas (orange). The figure shows that both waveshapes are similar, but as the formulas estimate the voltage after each reflection, the proposed method does not show the voltage decay between reflections. Therefore, the formulas represent a realistic worst-case representation of the voltage built up.

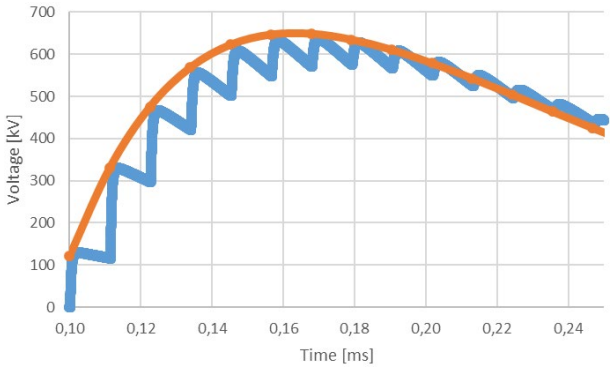

Figure 15 – Voltage at the cable sending end for a 1.2/50μs lightning impulse. Blue: PSCAD simulation; Orange: Proposed formulas plotted using smooth scatter from Excel

VI.2. Choice of lightning waveshape:

The choice of the representative lightning waveshape is a complex issue. Measurements and recommendations show a large rage of potential front and half-value times [7], [22], [23]. Many insulation coordination studies use the 1.2/50 μs double exponential waveshape, because it is the FFO standard voltage shape [12], even if it is not the most representative for lightning.

The authors do not attempt to recommend the waveshape that should be used to represent the lightning surge. Instead, the validation of the proposed formulas was made for multiple standard waveshapes and for a lognormal distribution of 100 front time and 10 half-value times based on data from [7] and [12]. The validation showed acceptable results, with some notable exceptions for extreme cases. It is up to the readers to select the waveshape that they find most suitable.

VI.3. Subsequent strokes:

Generally, subsequent strokes have lower current magnitudes than the first stroke, but might sometimes be larger than the first stroke, because the two current magnitudes are independent. The median peak current of a first stroke is 2-3 times larger than that of subsequent strokes and the typical procedure in insulation coordination studies is to consider only the first stroke [7], [24]. As the objective of the paper is to have a screening tool for engineering studies, only typical procedures are accounted and subsequent strokes are not considered in this paper.

If of interest, it should be noticed that subsequent strokes have similar waveshape and faster front times than first strokes. Thus, the proposed formulas might be used with subsequent strokes.

VI.4. Ground resistivity:

All simulations considered a ground resistivity of 100 Ω.m. The complex penetration depth was simplified when calculating the surge impedance of an OHL and it was demonstrated that the simplification has a large impact when estimating the OHL inductance, but a minor one when estimating the overvoltage due to shielding failure. A demonstration was done with a 10000 Ω.m soil resistivity, which lead to a 21% error in the inductance value, but only 4% in the peak overvoltage.

Table 1 presents the intermediate steps of this demonstration, considering an unrealistic shielding failure for a lightning current of 200 kA and a ground resistivity of 10000 Ω.m; a 1.2x50 μs impulse is considered, the cable is 1 km long, it is open at the opposite end and without surge arresters. It can be concluded that the formulas account for the soil resistivity when necessary and neglect it when it has a small impact in the voltage magnitude.

Table 1 – Estimation of different parameters considering penetration depth and with simplified expression. For the peak voltage, (x) is the number of the reflection

Variable	Simplified	With Penetration Depth	Diff. [%]	Simul.
L	6.308×10^{-6}	7.98×10^{-6}	21	
Surge Impedance OHL	171.3	191.6	11	
Coefficient OHL-cable: Eq. 8 (part I)	0.266	0.241	10.3	
Coefficient Cable-Cable: Eq. 10–k_{send} (Part I)	0.734	0.759	3.2	
Peak voltage [kV] (1)	13227	13356	1	13897
Peak voltage [kV] (2)	19038	19336	2	19289
Peak voltage [kV] (3)	22767	23264	2	22783
Peak voltage [kV] (4)	24914	25615	3	24859
Peak voltage [kV] (5)	25875	26769	3	25858
Peak voltage [kV] (6)	25962	27027	4	26065
Peak voltage [kV] (7)	25420	26629	5	25697

The impact of the high frequency of a lightning surge on the behaviour of the grounding system is another relevant question. To include frequency-dependence of the grounding system would increase the complexity of the method substantially. The objective of the method is to propose a simple screening method and the ground frequency dependence has a favourable effect for high frequencies by reducing the grounding impedance [25]. Thus, frequency-dependence of the soil is not considered, because it leads to a simpler method and more conservative results.

If desired, one option is to select a target frequency and to use one of the formulas available in the literature [25]-[28]. However, this approach would still be problematic for a screening tool, as it requires information about the grounding system, it increases the complexity of the estimation procedure and there would still be inaccuracies as multiple frequencies are present in a lightning surge.

VI.5. Shielding failure:

A shielding failure should be the worst-case scenario, as it means the highest stress to a cable insulation. The equations and the simulations show that the shorter the cable, the larger the voltage build-up. The exact magnitude depends on the lightning impulse, the attenuation along the cable and the relation between the surge impedances of cable and OHLs or other components connected to the cable terminal. If the only parameter changing is the cable length, some behaviours are observed if a surge arrester is not installed:

- The number of reflections required for reaching the peak overvoltage is approximately inversely proportional to the length (e.g. if a 1 km cable has 8 reflections before maximum overvoltage, a 2 km cable expects 4 reflections). The relation is not perfect, but it provides a good approximation, because of the explanation provided in the third bullet point;
- A corollary of the previous bullet point is that the maximum overvoltage is at approximately the same time instant, even if the length changes (the time-instant must correct to match the reflection and the cable must be short enough so that the maximum overvoltage is not at the first reflection);
- The variation of the voltage magnitude between reflections around maximum overvoltage is low. This is explained, as around this time period, the increasing voltage from the injected wave is mostly cancelled by the decreasing magnitude of the wave entering the cable and the attenuation of previous reflections.

Surge arrester are often installed at OHL-cable junction for protecting the cable, with a strong impact on the waveforms. The voltage no longer builds up for several reflections, as the surge arrester shaves the voltage. As a result, the maximum overvoltage is expected at the first reflections for lightning current magnitudes associated to shielding failure. Additionally, the presence of a surge arrester means that the cable length and the lightning current magnitude have a smaller impact on the maximum overvoltage, which is now mostly defined by the surge arrester characteristic, because it operates in the high-current region.

The energy dissipated at the surge arrester is a key parameter and the reflections at the cable terminations lead to an increase of the energy dissipated for short cable sections. Figure 16 shows the energy absorbed by a surge arrester for different cable lengths, both for an unloaded system and for a peak phase voltage at the lightning instant. The figure shows the large impact that the cable length has in the energy absorbed by the surge arrester and the need to account for the multiple reflections.

The possibility of multiple lightning impulses flowing into the surge arrester in a short-period time is not considered in this paper. This is no different from when protecting other pieces of equipment, but the larger energy absorbed due to the cable short length makes this situation even more challenging in areas with high keraunic indices.

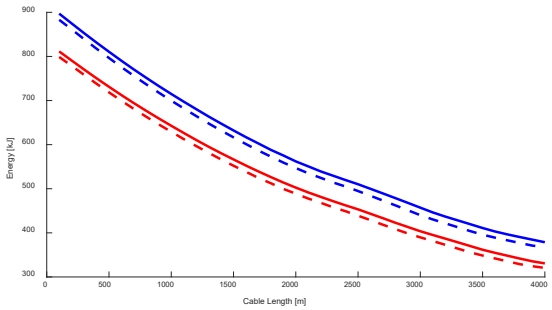

Figure 16 – Energy absorbed by the surge arrester for different cable lengths. Red: Unloaded system; Blue: Peak voltage at the phase at lightning instant. Solid lines: 1.2/50 µs impulse; Dashed lines: 2.6/50 µs impulse

VII. Conclusions

As the number of hybrid cable-OHL lines increases, the importance of lightning surges propagating into cables becomes more relevant. The estimation of the overvoltage for short cable sections is of special interest, because of the numerous reflections that occur. Part I of this work developed equations for a fast estimation of the voltage at a cable core, with and without surge arrester, in case of shielding failure. These equations can be implemented in a simple and direct manner with minimum data requirements for a fast screening of potential problems.

The simulation of different lightning impulse waveforms and different cable lengths shows that voltage build-up happens for short cable sections,. Surge arresters can limit the voltage build up, but more energy is to be absorbed by the surge arrestor for short cable sections.

In general, the formulas provide accurate estimations for the majority of scenarios, but the error increases in some situations. For shielding failure and no surge arrester, the error increases when the length of the lightning impulse front time increases. In the test cases, the error was below 10% for 85% of the front times recommended by [7] and [12], but it became rather large for front times longer than 15µs. The error is also larger if the time-to-half is similar to the front time. For shielding failure and surge arrester, the faster the front time, the larger the error. The error from the estimation formula was inferior to 8% to all tested cased and to 5% for 70% of the cases.

Part II of the paper presents equations for a fast estimation of the voltage at a cable sheath, in case the earth wire attracts the lightning surge.

VIII. References

[1]. T. E. McDermott, “Using IEEE Flash to estimate transmission and distribution line lightning performance”, IEEE PES T&D, 2012

[2]. IEEE-Flash [Online]. Available at: sourceforge.net/projects/ieeeflash (as of March 2021)

[3]. F Faria da Silva, Kasper S. Pedersen, Claus L. Bak, “Lightning in hybrid cable-overhead lines and consequent transient overvoltages”, International Conference on Power System Transients, 2017

[4]. L. Colla, F. M. Gatta, A. Geri, S. Lauria, “Lightning Overvoltages in HV-EHV “Mixed” Overhead-Cable Lines”, International Conference on Power System Transients, 2007

[5]. Thor Henriksen, “Maximum lightning overvoltage along a cable due to shielding failure”, Electric Power System Research 77, 2007

[6]. Thor Henriksen, Bjørn Gustavsen, Georg Balog, Ulf Baur, “Maximum Lightning Overvoltage Along a Cable Protected by Surge Arresters”, IEEE Transactions on Power Delivery, Vol. 20, 2005

[7]. CIGRE WG C4.407, “Lightning Parameters for Engineering Applications”, Cigré, 2013

[8]. CIGRE WG 33.01, “Guide to Procedures for Estimating the Lightning Performance of Transmission Lines”, Cigré, 1991

[9]. C. Gary, “Approche complète de la propagation multifilaire en haute fréquence par utilisation des matrices complexes”. EDF Bulletin de la Direction des Études et Recherches, Série B-Réseaux Electriques Matériels Électriques 1976

[10]. F. Faria da Silva, “Simplified formulae for the estimation of the positive-sequence resistance and reactance of three-phase cables for different frequencies”, UPEC 50th, 2015

[11]. Ametani, Ohno, Nagaoka, “Cable System Transients - Theory, Modeling and Simulation” Wiley & Sons, 2015

[12]. IEEE Std 1410-2010, “IEEE Guide for Improving the Lightning Performance of Electric Power Overhead Distribution Lines”, IEEE Power & Energy Society, 2011

[13]. K. Berger, R. B. Anderson, H. Kröninger, ”Parameters of Lightning Flashes”, Electra N. 41, 1975

[14]. IEEE WG 3.4.11, “Modelling of metal oxide surge arresters”, IEEE Transaction on Power Delivery, Vol. 7, 1992

[15]. CIGRE WG 33.06, “Metal Oxide Arresters in AC Systems”, Cigré, 1991

[16]. P. Pinceti, M. Giannettoni, "A simplified model for zinc oxide surge arresters", IEEE Transactions on Power Delivery, Vol. 14, 1999
[17]. F. Fernandez, R. Diaz, "Metal oxide surge arrester model for fast transient simulations", International Conference on Power System Transients, 2003
[18]. P. N. Mikropoulos, T.E. Tsovilis, "Lightning attachment models and maximum shielding failure current of overhead transmission lines: implications in insulation coordination of substations", IET Generation, Transmission & Distribution, Vol. 4, 2010
[19]. CIGRE WG C4.26, "Evaluation of Lightning Shielding Analysis Methods for EHV and UHV DC and AC Transmission Lines", Cigré, 2017
[20]. CIGRE WG B1.05, "Transient Voltages Affecting Long Cables", CIGRE, 2005
[21]. IEC 60071-2:2018, "Insulation co-ordination – Part 2: Application guidelines", IEC, Edition 4.0, 2018
[22]. Jun Takami, Shigemitsu Okabe, "Observational Results of Lightning Current on Transmission Tower", IEEE Transactions on Power Delivery Vol. 22, No. 1; 2007
[23]. Shigemitsu Okabe, Jun Takami, Toshihiro Tsuboi, Genyo Ueta, Akihiro Ametani, Kunihiko Hidaka, "Discussion on Standard Waveform in the Lightning Impulse Voltage Test", IEEE Transactions on Dielectrics and Electrical Insulation Vol. 20, No. 1; 2013
[24]. Andrew R. Hileman. Insulation Coordination for Power Systems. Taylor & Francis Group, 1st edition, 1999. ISBN-13: 978-0-8247-9957-1 (page 267)
[25]. CIGRE WG C4.33, "Impact of soil-parameter frequency dependence on the response of grounding electrodes and on the lightning performance of electrical systems", CIGRE, 2019
[26]. Silverio Visacro, Rafael Alipio, "Frequency Dependence of Soil Parameters: Experimental Results, Predicting Formula and Influence on the Lightning Response of Grounding Electrodes", IEEE Transactions on Power Delivery, Vol. 27, No. 2, 2012
[27]. C. L. Longmire, and K. S. Smith, "A universal impedance for soils," Topical Report for Period July 1– September 30, Defense Nuclear Agency, Santa Barbara, California, 1975
[28]. M. A. Messier, "The Propagation of an electromagnetic Impulse Through Soil: Influence of Frequency Dependent Parameters", MRC-N-415, Mission Research Corporation, Santa Barbara, 1980

IX. Appendix A

All simulations were done in PSCAD/EMTDC. The cables and OHLs were modelled using geometric frequency-dependent models, with the data from Table A.1 and Table A.2, respectively. Figure A.1 shows the position of the phase conductors and earth wires for the OHL, as well as the thickness and position of the core, insulation, sheath and outer insulation for the cable. Figure A.2 shows the schematic for shielding failure simulations shown in chapters IV and V.

Table A.1 – Cable data

Layer	Radius (mm)	Properties
Conductor	27.7	$\rho=3.5917\text{x}10^{-8}$ [Ω.m]
Insulation	58.2	$\varepsilon_r=2.87$
Sheath	59.0	$\rho=2.826\text{x}10^{-8}$ [Ω.m]
Outer Insulation	65.0	$\varepsilon_r=2.3$
Ground		ρ=100 [Ω.m]

Table A.2 – OHL data

Layer	Radius (mm)	Properties
Phase	18.085	DC_Res=0.04277 [Ω/km]
Bundle	3 conductors	d=0.4 [m]
Earth wire	8	DC_Res=0.299 [Ω/km]
Dist. phases		d=13.1 [m]

Ground		ρ=100 [Ω.m]

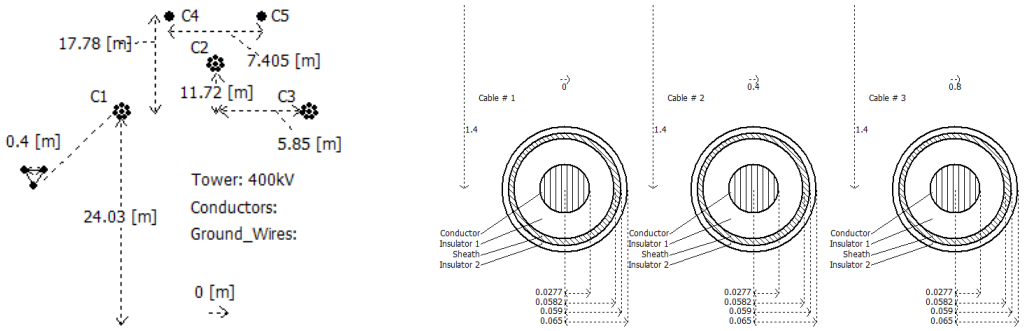

Figure A.1 – Geometric data on OHL (left) and cable (right)

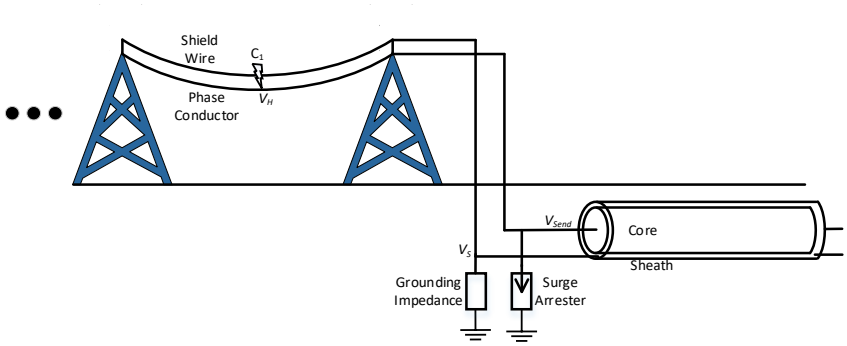

Figure A.2 – Schematic for the performed simulation: C_1 corresponds to a shielding failure. Surge arrester is not considered for the cases of chapter IV

X. Appendix B

Derivation of Equation (14) - W_{Front}

The deduction of (14) is done in (24) for the 2nd reflection, where the voltage is reflected at the cable junction point, after being reflected once at the sending end and twice at the receiving end. In (24), this is represented by the first three terms and the last four terms of the polynomial between brackets, respectively.

$$W_{Front}(2) = \frac{V_{H\_C}}{e^{n(2A\cdot l_C)}} \cdot \left(k_{Rec}\cdot k_{Rec}\cdot k_{Send} + k_{Rec}\cdot k_{Rec}\cdot k_{Send}\cdot k_{Send}\right) \tag{24}$$

Equation (24) can simplify into (25). For the following reflections, the power of 2 in (25) is replaced by the number of the reflection, resulting in (14).

$$\begin{aligned} W_{Front}(2) &= \frac{V_{H\_C}}{e^{n(2A\cdot l_C)}} \cdot {k_{Rec}}^2 \cdot k_{Send}\left(1+k_{Send}\right) \\ \Leftrightarrow W_{Front}(2) &= \frac{V_{H\_C}}{e^{n(2A\cdot l_C)}} \cdot \left(k_{Rec}\cdot k_{Send}\right)^2 \left(1+\frac{1}{k_{Send}}\right) \end{aligned} \tag{25}$$

Derivation of Equation (22) – W_{Front_Arr}

Contrary to the case without surge arrester, the value of k_{send} is not constant, but a function of the current flowing into the surge arrester that changes for every reflection. The value k_{send_Arr} for reflection n is then the multiplication of the previous k_{send}. Example, $k_{send\_Arr}(3) = k_{send}(2).k_{send}(1)$ and $k_{send}(2) \neq k_{send}(1)$, because of the surge arrester.

$$W_{Front\_Arr}(3) = \frac{V_{H\_C}}{e^{n(2A\cdot l_C)}} \cdot \left(k_{Rec}\cdot k_{Rec}\cdot k_{Rec}\cdot k_{Send}(1)\cdot k_{Send}(2) + k_{Rec}\cdot k_{Rec}\cdot k_{Rec}\cdot k_{Send}(1)\cdot k_{Send}(2)\cdot k_{Send}(3)\right) \tag{26}$$

$$W_{Front\_Arr}(3) = \frac{V_{H\_C}}{e^{n(2A \cdot l_C)}} \cdot k_{Rec}{}^{3} \left(k_{Send}(1) \cdot k_{Send}(2) + k_{Send}(1) \cdot k_{Send}(2) \cdot k_{Send}(3) \right)$$

$$\Leftrightarrow W_{Front\_Arr}(3) = \frac{V_{H\_C}}{e^{n(2A \cdot l_C)}} \cdot k_{Rec}{}^{3} \cdot \left(k_{Send}(1) \cdot k_{Send}(2) \right) \cdot \left(1 + k_{Send}(3) \right) \tag{27}$$

$$\Leftrightarrow W_{Front\_Arr}(3) = \frac{V_{H\_C}}{e^{n(2A \cdot l_C)}} \cdot k_{Rec}{}^{3} \cdot k_{Send\_Arr}(3) \cdot \left(1 + k_{Send}(3) \right)$$

For a reflection n, the multiple instance of the number 3 in (27) are replaced by n (22).